AGU PUBLICATIONS

Journal of Geophysical Research: Atmospheres

Supporting Information for

Modeling study of the air quality impact of record-breaking Southern California wildfires in December 2017

Hongrong Shi[1], Bin Zhao[1,*], Zhe Jiang[1,*], Zhijin Li[2], Yang Chen[3], Yu Gu[1], Jonathan H. Jiang[2], Meemong Lee[2], Kuo-Nan Liou[1], Jessica L. Neu[2], Vivienne H. Payne[2], Hui Su[2], Yuan Wang[4], Marcin Witek[2], and John Worden[2]

1. Joint Institute for Regional Earth System Science & Engineering, University of California, Los Angeles, California
2. Jet Propulsion Laboratory, California Institute of Technology, Pasadena, California
3. Department of Earth System Science, University of California, Irvine, California
4. Division of Geological and Planetary Sciences, California Institute of Technology, Pasadena, California

* Correspondence Author

Hongrong Shi and Bin Zhao contribute equally to this paper.

Contents of this file

Text S1. Supplementary information for fire emission estimate and plume-rise treatment

In this study, the carbon density used in fire emission estimate was derived from *Olson et al.* [2000] and Houghton et al. [2001] for the year 2000. To investigate the vegetation change from 2000 to 2017 and the potential impact on fire emission estimate, we examine the trend in NDVI (normalized difference vegetation index) which roughly indicates vegetation density. We obtain NDVI data from the MODIS/Terra Vegetation Indices Monthly L3 Global 1km SIN Grid V006 product. We focus on the monthly averaged NDVI in November, which represents the carbon density just before the outburst of the Thomas fire in December. As shown in Table S1, the differences between $NDVI_{Nov,2000}$ and $NDVI_{Nov,2017}$ are less than 10% either over a small region where the Thomas fire took place (34.25–34.55 N, 119.05–119.65 W), or over a larger surrounding region (33.2–35.2 N, 118.2–120.6 W). Therefore, we didn't update the 2000 carbon density to 2017 in this study.

To examine whether all fire pixels are effectively detected by VIIRS during the initial period of the fire (before December 9), we have compared the VIIRS-detected active fire pixels (used to estimate fire emissions in the V_VIIRS scenario) with the fire perimeter from Inciweb (https://inciweb.nwcg.gov/incident/maps/5670/). Figure S4 shows the comparison results on December 6 and December 9. On December 6, the spatial ranges of the Thomas fire given by the two sources agree very well with each other. On December 9, the spatial ranges still match generally, but VIIRS did not detect active fires in some areas where fires were identified by Inciweb, probably because these areas had transitioned to the smoldering phase by December 9 and no flames existed any more. The undetected fire pixels may lead to an underestimate of fire-induced $PM_{2.5}$ concentrations. However, since the largest underestimate occurs around December 6 when VIIRS and Inciweb match very well, the undetected fires may not be the main cause of the large underestimate at the beginning stage of the fire.

To test whether the plume-rise treatment is reasonable, we compare simulated vertical distribution of primary aerosol emissions from the December 2017 fire event (V_VIIRS scenario) with that retrieved by MISR [*Martin et al.*, 2018], as shown in Fig. S1. Since the MISR plume height product is not available in December 2017 (the available time range is 2008-2010 or 2008-2011, depending on product version), we estimate a typical plume vertical distribution in the Thomas fire area and use it to evaluate simulation results. No active fires were detected by MISR in December of 2008-2011 near the Thomas fire location (33.2–35.2 N, 118.2-120.6 W). Hence the typical plume vertical distribution in this area is estimated by averaging all fire plumes in North America in winter (DJF) for shrubland, the vegetation type at the scene of the Thomas fire. Fig. S1 shows that the plume vertical distributions from the model and MISR agree fairly well (correlation coefficient = 0.943), except that the model predicts more fire emissions at 250-500 m and less emissions at 0-250 m compared with MISR. Therefore, the plume rise estimate in this study appears to be reasonable overall. *Archer-Nicholls et al.* [2015] found that WRF-Chem predicted layers of elevated aerosol loadings at high altitude (4–8 km) over tropical forest regions, while flight measurements showed a sharp decrease above 2–4 km altitude. This problem is not observed in our simulation over southern California.

Text S2. Impact of aerosol radiative effect on meteorology and chemistry simulation

We have done an additional simulation (V_VIIRS_noFd) which is the same as the V_VIIRS scenario except that the aerosol direct effect is removed. The differences between the V_VIIRS and V_VIIRS_noFd scenarios represent the impact of the aerosol direct effect, as illustrated in Fig. S9. We have not examined the aerosol indirect feedback effect because nearly all clouds during the simulation period are located above 7 km (Fig. S8) which are not likely to be significantly affected by fire emissions that are injected below 3 km (Fig. S1). Fig. S9 shows that the inclusion of aerosol direct effect attenuates surface shortwave radiation, especially over the nearby and downwind region of the wildfire, and over the Central Valley which is mainly polluted by anthropogenic emissions. The subsequent feedback on meteorology and aerosol pollution is distinctly different in the above two regions. In the Central Valley, the attenuated shortwave radiation leads to a reduction in surface temperature (T), planetary boundary layer (PBL) height, which in turn increases surface $PM_{2.5}$ concentrations. Such a positive feedback loop has been demonstrated by many previous studies [*Wang et al.*, 2014; *Zhou et al.*, 2019]. In the nearby and downwind region of the fire, however, little changes in T and PBL height are observed, and the changes in $PM_{2.5}$ concentrations are positive in most areas but can be negative in some areas. The small and uneven response in this region is likely induced by the strong Santa Ana wind and complicated meteorological conditions, which warrants further in-depth study in the future.

Table S1. The monthly averaged NDVI in November, 2000 and 2017 over a small region where the Thomas fire takes place (34.25–34.55 N, 119.05–119.65 W), and over a larger surrounding region (33.2–35.2 N, 118.2–120.6 W).

	34.25–34.55 N, 119.05–119.65 W	33.2–35.2 N, 118.2–120.6 W
$NDVI_{Nov,2000}$	0.49425	0.26719
$NDVI_{Nov,2017}$	0.44653	0.25363

Table S2. Model performance of meteorological parameters in the V_VIIRS_nudging scenario as compared to observational data from the National Climatic Data Center (NCDC).

Variable	Index	Value	Ref[1]	Variable	Index	Value	Ref
Wind Speed (m/s)	Mean Observation	4.17		Temperature (K)	Mean Observation	276.53	
	Mean Prediction	3.54			Mean Prediction	276.04	
	Bias	-0.64	≤±0.5		Bias	-0.49	≤±0.5
	Gross Error	1.57	≤2		Gross Error	2.78	≤2
	IOA[2]	0.75	≥0.6		IOA	0.93	≥0.8
Wind Direction (deg)	Mean Observation	286.45		Humidity (g/kg)	Mean Observation	2.98	
	Mean Prediction	276.10			Mean Prediction	2.84	
	Bias	2.86	≤±10		Bias	-0.14	≤±1
	Gross Error	43.35	≤30		Gross Error	0.68	≤2
					IOA	0.81	≥0.6

[1]The reference values are taken from *Emery et al.* [2001].

[2]IOA: Index of Agreement

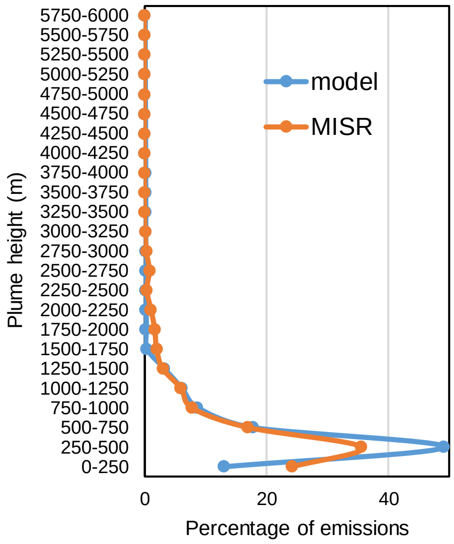

Figure S1. Percentages of modeled fire smoke injection heights for the December 2017 fire event (V_VIIRS scenario, 33.2–35.2 N, 118.2–120.6 W) and MISR-based fire smoke injection heights for shrubland in North America in winter (DJF), 2008, 2009 and 2010.

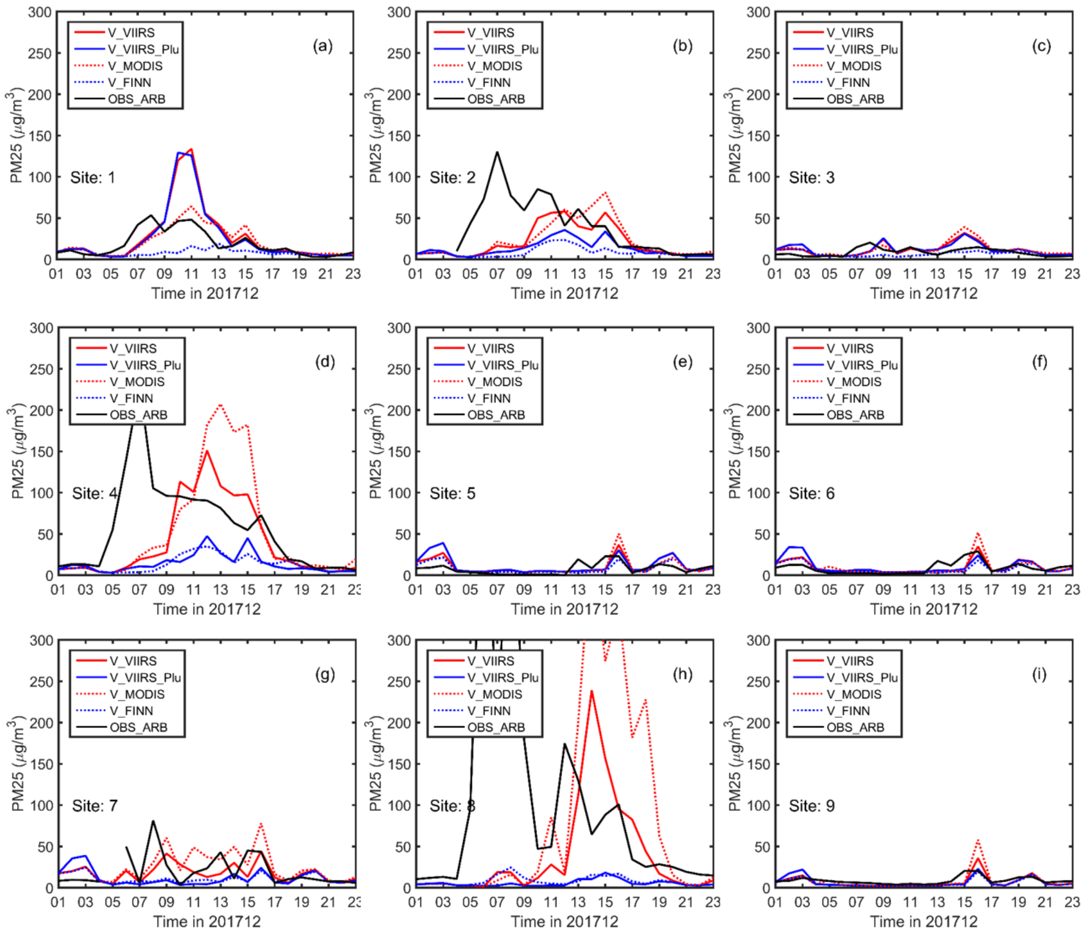

Figure S2. Time series of daily average $PM_{2.5}$ concentrations at 9 sites around wildfires from four scenarios during December 1 to 23, 2017.

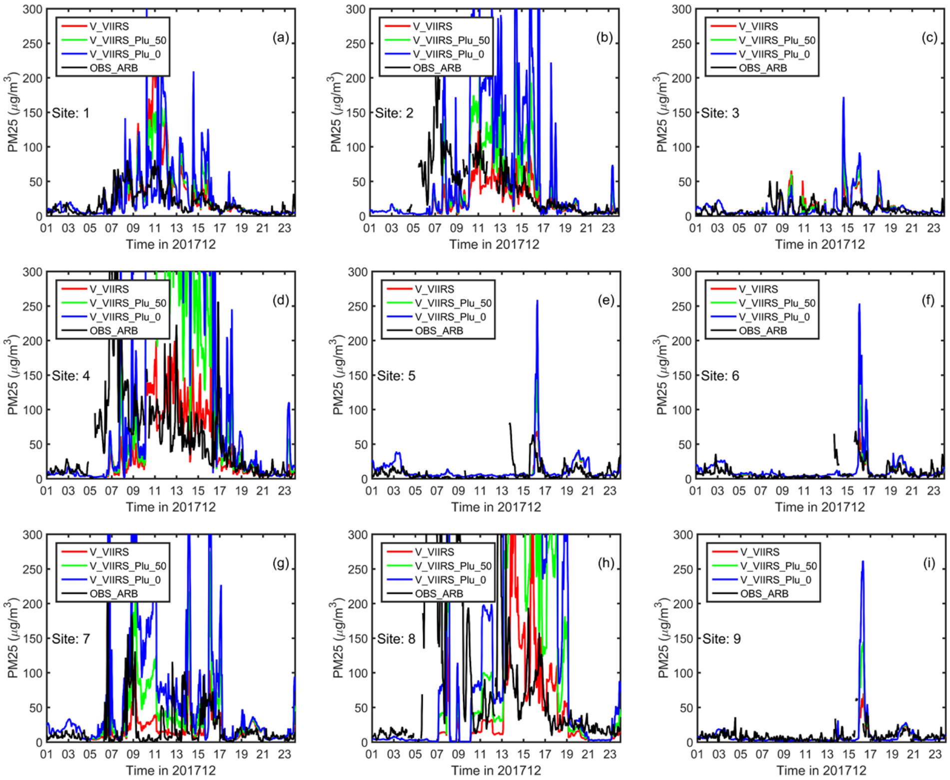

Figure S3. Time series of $PM_{2.5}$ concentrations at 9 sites around wildfires during December 1 to 23, 2017. The black line is observed hourly $PM_{2.5}$ concentration. The red, green, and blue lines are simulation results assuming different splits between flaming and smoldering phases.

December 6 December 9

VIIRS-detected active fire pixels used in this study

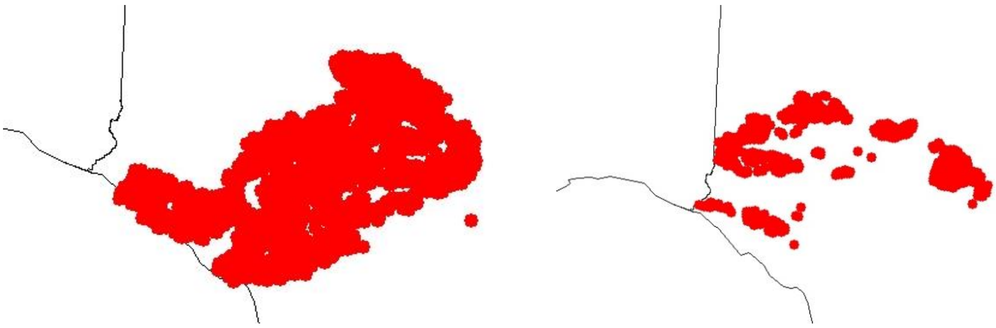

Inciweb

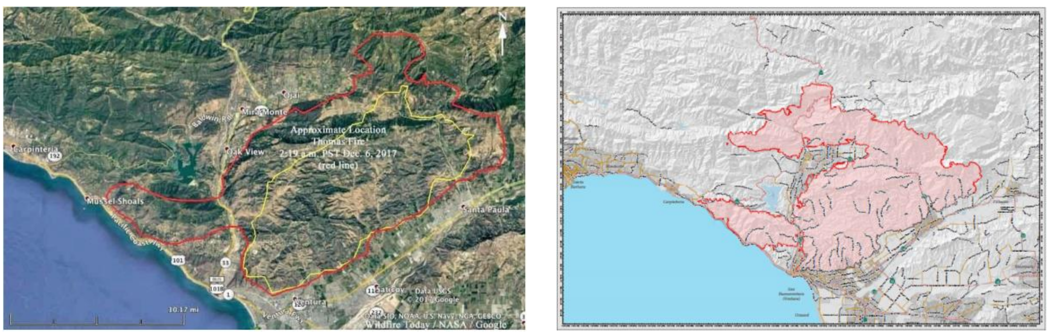

Figure S4. VIIRS-detected active fire pixels used to estimate emissions in the V_VIIRS scenario (top) and fire perimeter from Inciweb (bottom) on December 6 (left) and December 9 (right).

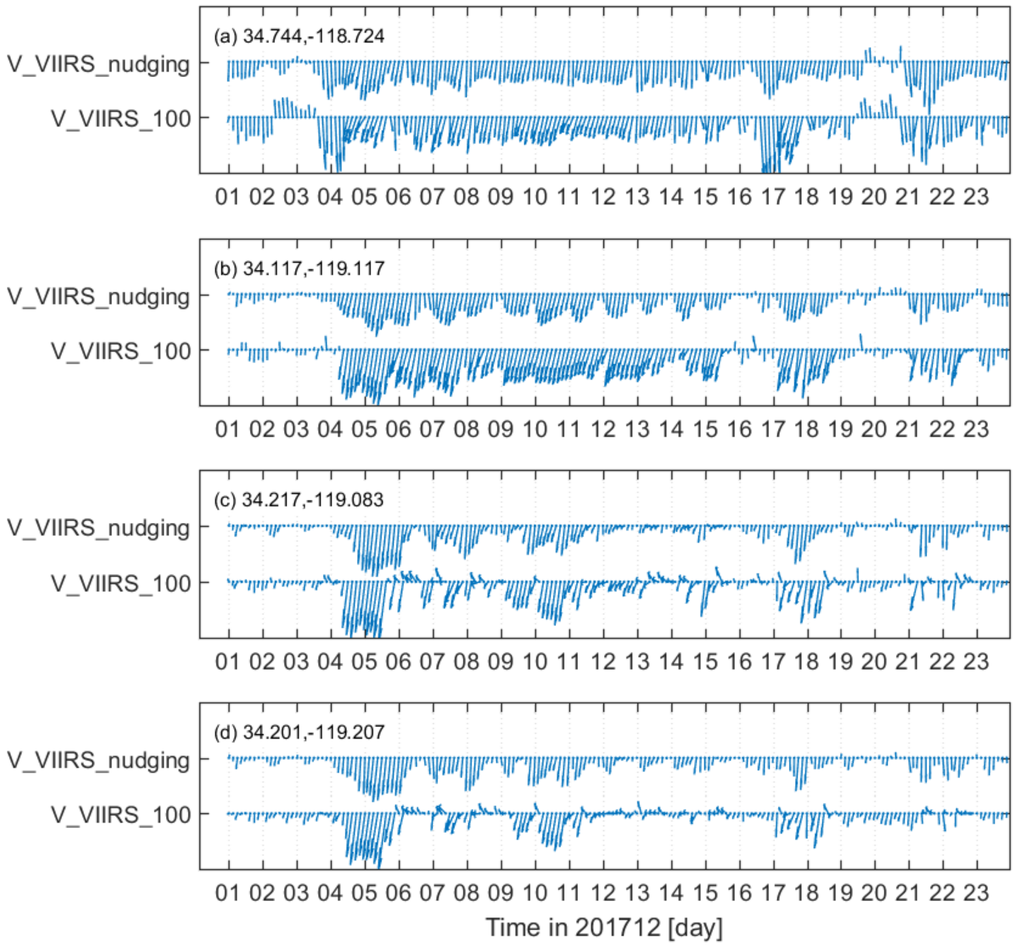

Figure S5. Comparison between surface observed wind fields from NCDC and WRF-Chem simulations in the V_VIIRS_100 and V_VIIRS_nudging scenarios at 4 sites near the fires.

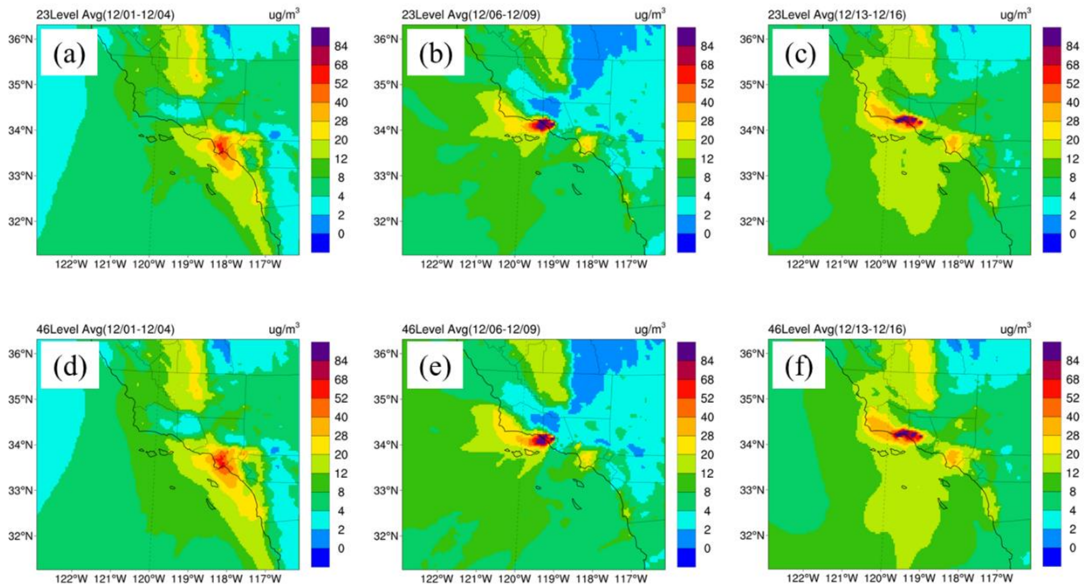

Figure S6. Spatial distributions of surface $PM_{2.5}$ concentrations from the simulations with (a-c) 23 levels and (d-f) 46 levels during three stages of the fire event: (a, d) the pre-Santa Ana wind stage, (b, e) the Santa Ana wind stage, and (c, f) the post-Santa-Ana wind stage.

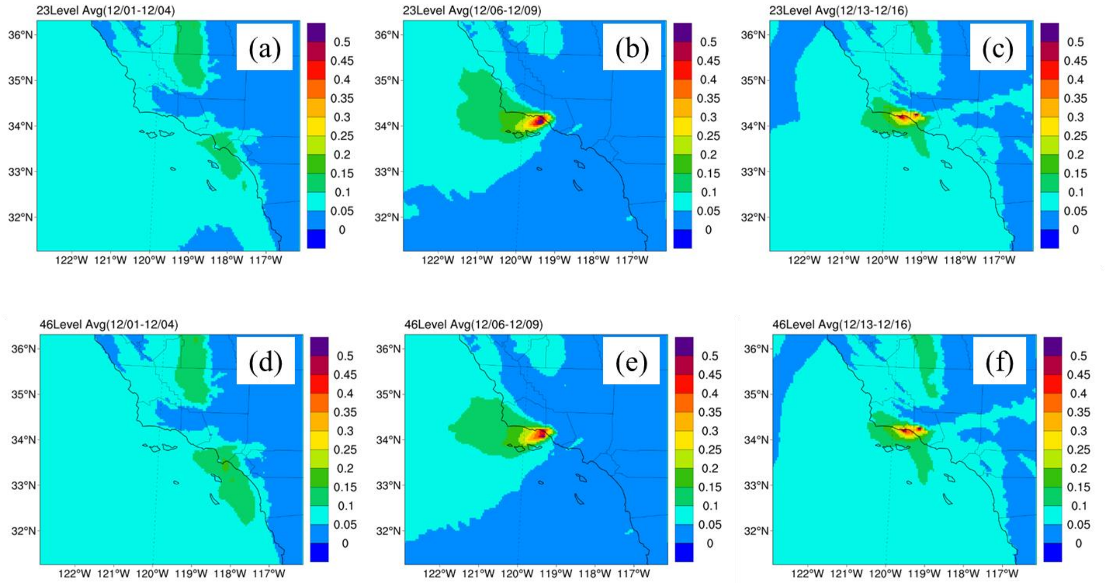

Figure S7. Spatial distributions of AOD from the simulations with (a-c) 23 levels and (d-f) 46 levels during three stages of the fire event: (a, d) the pre-Santa Ana wind stage, (b, e) the Santa Ana wind stage, and (c, f) the post-Santa-Ana wind stage.

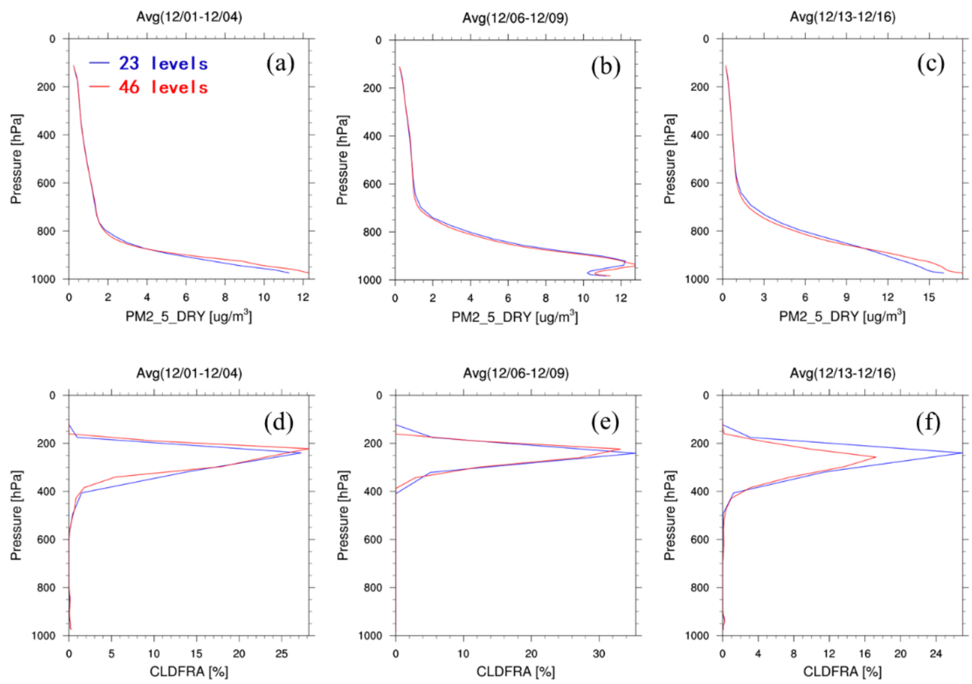

Figure S8. Vertical distributions of (a-c) $PM_{2.5}$ concentrations and (d-f) cloud fraction from the simulations with 23 and 46 levels during three stages of the fire event: (a, d) the pre-Santa Ana wind stage, (b, e) the Santa Ana wind stage, and (c, f) the post-Santa-Ana wind stage. The data are horizontally averaged over a region near the fire (33.2-35.2 N, 120.6-118.2 W).

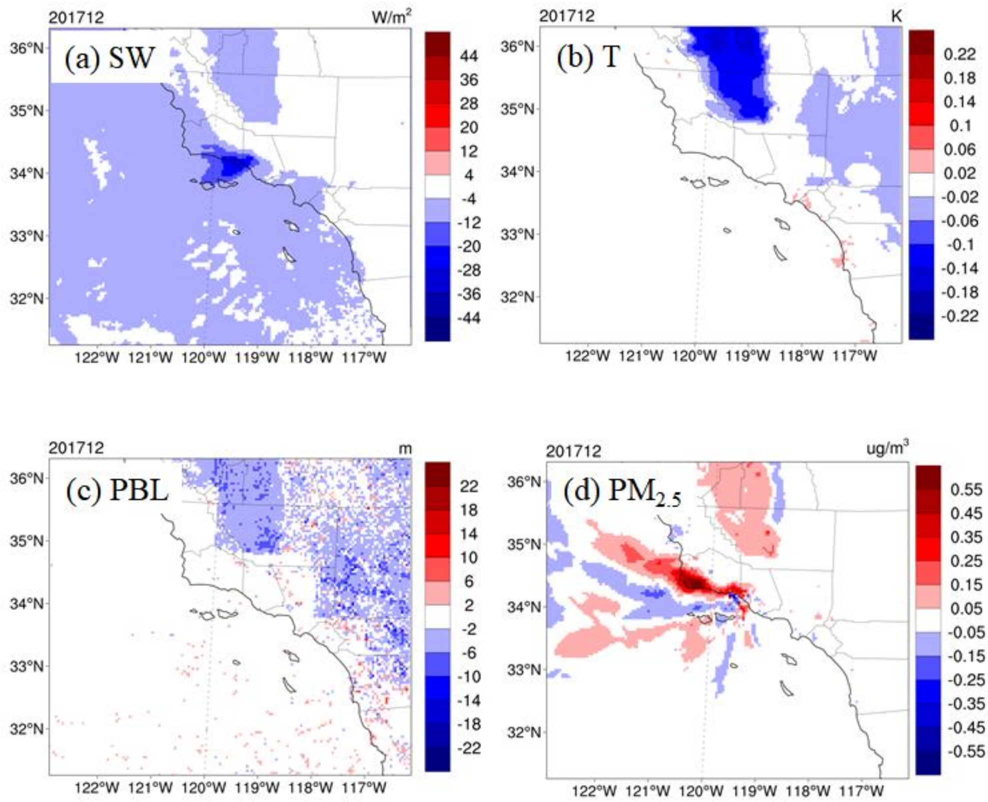

Figure S9. Difference between the V_VIIRS and V_VIIRS_noFd (V_VIIRS without aerosol direct feedback) scenarios during the fire period (Dec 5 to Dec 18): (a) surface shortwave irradiance (SW), (b) surface temperature (T), (c) planetary boundary layer (PBL) height, and (d) surface $PM_{2.5}$ concentrations.

Reference

Archer-Nicholls, S., et al. (2015), Characterising Brazilian biomass burning emissions using WRF-Chem with MOSAIC sectional aerosol, *Geosci Model Dev*, *8*(3), 549-577.

Emery, C., E. Tai, and G. Yarwood (2001), Enhanced meteorological modeling and performance evaluation for two texas episodes. Report to the Texas Natural Resources Conservation Commission*Rep.*, ENVIRON International Corporation, Novato, CA.

Houghton, R., K. Lawrence, J. Hackler, and S. Brown (2001), The spatial distribution of forest biomass in the Brazilian Amazon: a comparison of estimates, *Global Change Biology*, *7*(7), 731-746.

Martin, M. V., R. A. Kahn, and M. G. Tosca (2018), A Global Analysis of Wildfire Smoke Injection Heights Derived from Space-Based Multi-Angle Imaging, *Remote Sens-Basel*, *10*(10), 1609.

Olson, J., J. Watts, and L. Allison (2000), Major World Ecosystem Complexes Ranked by Carbon in Live Vegetation: A Database (Revised November 2000), available at https://cdiac.ess-dive.lbl.gov/ndps/ndp017.html*Rep.*, Oak Ridge National Laboratory, Oak Ridge, Tennessee, USA.

Wang, J. D., et al. (2014), Impact of aerosol-meteorology interactions on fine particle pollution during China's severe haze episode in January 2013, *Environ Res Lett*, *9*, 094002.

Zhou, M., L. Zhang, D. Chen, Y. Gu, T. M. Fu, M. Gao, Y. H. Zhao, X. Lu, and B. Zhao (2019), The impact of aerosol-radiation interactions on the effectiveness of emission control measures, *Environ Res Lett*, *14*(2), 024002.